Learning spatio-temporal properties of hippocampal place cells

Author Names and Affiliations: Yanbo Lian[1], Anthony N. Burkitt[1]

[1] Department of Biomedical Engineering, The University of Melbourne, Melbourne, VIC, 3010, Australia

Correspondence: {yanbo.lian, aburkitt}@unimelb.edu.au

Number of pages: 29

Number of figures: 7

Acknowledgements: This work received funding from the Australian Government, via grant AUS-MURIB000001 associated with ONR MURI grant N00014-19-1-2571.

Conflict of interest statement: The authors declare no competing financial interests.

Abstract

Hippocampal place cells have spatio-temporal properties: they generally respond to a single spatial position of a small environment; in addition, they also display a temporal property, the theta phase precession, namely that the phase of spiking relative to the theta wave shifts from the late phase to early phase as the animal crosses the place field. Grid cells in layer II of medial entorhinal cortex (MEC) also have spatio-temporal properties similar to hippocampal place cells, except that grid cells respond to multiple spatial locations that form a hexagonal pattern. Other non-grid spatial cells are also abundant in the entorhinal cortex (EC). EC is the upstream that projects strongly to the hippocampus, many EC-hippocampus models have been designed to explain how the spatial property of place cells emerges. However, there is no learning model explaining how the temporal properties of hippocampal place cells emerge from the EC input. A learning model is presented here based on non-negative sparse coding in which we show that the spatial and temporal properties of hippocampal place cells can be simultaneously learnt from EC input: both MEC grid cells and other EC spatial cells contribute to the spatial properties of hippocampal place cells while MEC grid cells contribute to the temporal properties of hippocampal place cells.

1 Introduction

In an early electrophysiological experiment involving freely behaving rats, O'Keefe and Dostrovsky (1971) discovered place cells, the principal cells in the hippocampus. Place cells, as suggested by their name, have the spatial property of responding selectively to places in the external environment; namely they generally respond to a particular location (called the place field) of the spatial environment O'Keefe and Dostrovsky (1971), although they may respond to multiple locations in a large environment (Park et al., 2011). In addition to the spatial properties of place cells, their temporal response properties, namely theta phase precession, was observed by O'Keefe and Recce (1993): the place cell fires spikes at progressively earlier phases of the local field potential theta rhythm (7-12 Hz) while the animal moves across the place field. Normally, the firing of an action potential starts at the late phase of the theta rhythm when the animal enters the place field and ends at the early phase when the animal exits the place field (O'Keefe and Recce, 1993).

Three decades after hippocampal place cells were discovered, Hafting et al. (2005) reported another type of

spatial cells, the grid cells, in the medial entorhinal cortex (MEC) that is an adjacent area to the hippocampus. Similar to the spatial property of place cells in the hippocampus, MEC grid cells are also selective to spatial locations of the environment, but each MEC grid cell responds to multiple spatial locations (each location is called a grid field) forming a hexagonal grid that tiles the entire environment (Hafting et al., 2005). Moreover, there is a diversity resulting from multiple hexagonal grids of different MEC grid cells that have different orientations, spacings and offsets (Stensola et al., 2012). Subsequently, MEC grid cells were also observed to have the temporal response property of theta precession: the firing of MEC grid cells begins at the late phase of the theta rhythm when the animal enters the grid field, the phase of firing shifts in a systematic way during the traversal of the grid field, and ends at the early phase when the animal exits the grid field (Hafting et al., 2008). Though the spatial property of place cells and MEC grid cells were discovered in an open environment (O'Keefe and Dostrovsky, 1971; Hafting et al., 2005), early studies primarily investigated theta precession on linear tracks (O'Keefe and Recce, 1993; Hafting et al., 2008). The phase precession of both place cells and MEC grid cells in the open environment was investigated in a later study by Jeewajee et al. (2014).

Hippocampal place cells and MEC grid cells can be considered as the "GPS units" of the brain and there is a close relationship between these two types of cells. Experimental studies indicate that input from the entorhinal cortex (EC) is the principal input to the hippocampus (Steward and Scoville, 1976; Tamamaki and Nojyo, 1993; Leutgeb et al., 2007; Zhang et al., 2013). Consequently, MEC grid cells along with other cells in EC are thought to provide spatial input for hippocampal place cells, so that they can have a specific place tuning. This has led to numerous feedforward EC-hippocampus models in which single place fields are generated from EC input, such as MEC grid cells or EC weakly spatial cells (Solstad et al., 2006; de Almeida et al., 2009; Rolls et al., 2006; Franzius et al., 2007b,a; Savelli and Knierim, 2010; Neher et al., 2017; Lian and Burkitt, 2021). Furthermore, Fiete et al. (2008) showed that this MEC grid cell structure represents an encoding scheme for position that is analogous to the residue number system (Soderstrand et al., 1986), which is a highly efficient and accurate method for place representation. On the other hand, place cells in CA1 of the hippocampus project back directly or indirectly to EC (Kloosterman et al., 2003; Naber et al., 2001; Slomianka et al., 2011), supporting a loop-like EC-hippocampus network structure. This loop-like structure has been adopted in some modelling studies to explain other spatial properties of place

and MEC grid cells such as global and rate remapping of place cells, and multisensory integration in MEC grid cells (Rennó-Costa and Tort, 2017; Li et al., 2020). Compared with the feedforward EC-hippocampus models, the loop-like models can also incorporate the effects on the spatial firing of MEC grid cells due to the feedback introduced in such models.

Separate from the link between the spatial property of place cells and MEC grid cells, some experimental studies also infer a link between the temporal properties of place cells and MEC grid cells. Hafting et al. (2008) discovered that MEC grid cells have hippocampus-independent phase precession and suggested that phase precession of hippocampal place cells might be inherited from EC. In a review paper, Bush et al. (2014) suggest that the theta phase precession of place cells is likely inherited from MEC grid cell input. Later in another study by Schlesiger et al. (2015), MEC was found to be necessary for the temporal properties of hippocampal neuronal activity, even when place cells maintain stable spatial firing. However, existing EC-hippocampus models only focus on the learning of spatial properties and there is no existing model that explicitly shows how the temporal properties of hippocampal place cells can be inherited from MEC grid cells through some form of Hebbian learning. We propose here a learning model in which the spatio-temporal properties of hippocampal place cells emerge through synaptic plasticity during navigation of a virtual rat in a 2D environment.

The learning model presented here is built upon our previous work that shows that the model based on non-negative sparse coding can learn an efficient hippocampal place map using EC input such as MEC grid cells and EC weakly spatial cells (Lian and Burkitt, 2021). In this paper, building upon the work of Jeewajee et al. (2014) and McClain et al. (2019), we construct a mathematical model of MEC spatio-temporal grid cells of a 2D environment. These MEC spatio-temporal grid cells, along with EC weakly spatial cells, form the input to modelled hippocampal place cells, and the connection between EC input cells (MEC grid cells and EC weakly spatial cells) and modelled hippocampal place cells are learnt during navigation of a virtual rat. After learning, the modelled hippocampal place cells display spatial and temporal properties that are similar to experimental data. Furthermore, after the learning process, modelled hippocampal place cells still maintain their spatial selectivity even when MEC spatio-temporal grid cells are inactivated, suggesting that the remaining EC weakly spatial cells give rise to the place fields of modelled hippocampal place cells. Combining our previous work showing that either MEC grid cells or EC weakly spatial cells can give rise

to the spatial tuning of hippocampal place cells (Lian and Burkitt, 2021), we complete the picture of how EC input contributes to the properties of hippocampal place cells from the perspective of synaptic plasticity; namely that hippocampal place cells learn the spatial property from both MEC grid cells and EC weakly spatial cells, and learn their temporal properties from MEC grid cells. The synaptic plasticity underlying the learning model here is based on the principle of sparse coding.

2 Materials and Methods

2.1 The environment and trajectory

The spatial environment used in this study is a 1m×1m square box where a virtual rat runs freely. Similar to the work by D'Albis and Kempter (2017), the running trajectory $\boldsymbol{r}_t$ is generated from the stochastic process described as

$$\frac{\mathrm{d}\boldsymbol{r}_t}{\mathrm{d}t} = v_t \left[\cos(\theta_t), \sin(\theta_t)\right] \text{ with } \theta_t = \sigma_\theta \omega_t, \tag{1}$$

where v_t is the speed sampled from an Ornstein-Uhlenbeck process with long-term mean $\bar{v}_t = v$, θ_t is the direction of movement, ω_t is a standard Wiener process, and σ_θ is the parameter that controls the tortuosity of the running trajectory.

When the virtual rat is running toward the wall and very close to the wall (within 2cm), the running direction of the rat (θ_t) is set to the direction parallel to the wall. If the rat location generated by Eq 1 falls outside of the environment, the stochastic process keeps running until a valid location is generated.

The running trajectory of the virtual rat is generated at 100 Hz, i.e., the position is updated after every 10 ms according to Eq 1. The long-term mean speed, v, is set to 30 cm/s. A summary of parameters and values used in the simulation can be found in Table 1.

2.2 Model of MEC spatio-temporal grid cells

MEC grid cells are found to have spatial and temporal properties, namely they are selective to a hexagonal grid of spatial locations (Hafting et al., 2005; Stensola et al., 2012) and their firing displays theta phase precession (Hafting et al., 2008). The spatial receptive fields of MEC grid cells can be characterised by the

Table 1: **Model symbols and parameters.**

Description (values)	**Symbol**
Tortuosity of the running trajectory (1)	σ_θ
Spatial location / running speed / running direction and at time t	$\boldsymbol{r}_t$ / v_t / θ_t
Long-term mean of the speed (30 cm/s)	v
Time step of the running trajectory (10 ms)	
Duration of the training / testing running trajectory (3600 s / 1200 s)	
Spatial location in the environment	$\boldsymbol{r}$
Spatio-temporal response at spatial location $\boldsymbol{r}$ at time t	$f(\boldsymbol{r}, t)$
Spatial receptive field	$f_s(\boldsymbol{r})$
Amplitude / centre / radius of the spatial receptive field	α_c / $\boldsymbol{r}_c$ / R
Phase modulation at spatial location $\boldsymbol{r}$ at time t	$f_\phi(\boldsymbol{r}, t)$
Level of phase modulation (uniformly sample from [0.8 1.2])	k_ϕ
Frequency of the theta rhythm (10 Hz)	F
Firing phase at location $\boldsymbol{r}$	$\phi(\boldsymbol{r})$
Entry phase of phase precession (uniformly sampled from [300° 340°])	ϕ_0
Phase change of phase precession (uniformly sampled from [300° 340°])	$\Delta\phi$
Projected centre / radius of the spatial receptive field onto running direction	$\boldsymbol{r}'$ / R'
Fitted spatial receptive fields of modelled hippocampal cells	$\hat{f}_s(\boldsymbol{r})$
Amplitude / centre / radius of the fitted spatial receptive field	$\hat{\alpha}_c$ / $\hat{\boldsymbol{r}}_c$ / $\hat{R}$
Fitted level of phase modulation	$\hat{k}_\phi$
Fitted frequency of theta rhythm	$\hat{F}$
Fitted phase of the temporal response	$\hat{\phi}$
Membrane time constant of modelled hippocampal cells (10 ms)	τ
Membrane potentials of modelled hippocampal cells	$\boldsymbol{u}$
Firing rates of modelled hippocampal cells	$\boldsymbol{s}$
Firing rates of EC input cells	$\boldsymbol{I}$
Excitatory connection: EC input cells to modelled hippocampal cells	$\mathbf{A}$
Firing threshold of modelled hippocampal cells (0.3)	β
Learning rate (0.01)	
Time step of computing modelled hippocampal place cells by Eq 7 (0.2 ms)	
Number of modelled hippocampal place cells in Scenario 1, 2 and 3 (100)	
Number of MEC spatio-temporal grid cells in Scenario 1, 2 and 3 (900)	
Number of EC weakly spatial cells in Scenario 2 and 3 (400)	

sum of three sinusoidal gratings (Solstad et al., 2006) or the sum of circular fields at different locations in the environment. However, there is no mathematical model that can capture the temporal properties of MEC grid cells. In order to investigate the question of whether the spatial and temporal properties of hippocampal place cells can be inherited from MEC grid cells via learning, we first need a mathematical model that can characterise both spatial and temporal properties of MEC grid cells.

Chadwick et al. (2015) and McClain et al. (2019) build a mathematical model for 1D place cells that have spatial and temporal properties, and Jeewajee et al. (2014) showed that theta phase precession of place cells depends on the running direction in 2D environment. Inspired by their work, we build a mathematical model of MEC spatio-temporal grid cells based on 2D spatio-temporal place cells. The fundamental idea is that the receptive field of each MEC spatio-temporal grid cell is seen as the combination of multiple grid fields located in the hexagonal grid where each grid field has spatio-temporal properties similar to a 2D spatio-temporal place cell.

Within the region of any receptive field, the firing rate at location $\boldsymbol{r}$ and time t is modelled as the product of a spatial receptive field and a phase modulation (McClain et al., 2019):

$$f(\boldsymbol{r}, t) = f_s(\boldsymbol{r}) \cdot f_\phi(\boldsymbol{r}, t). \tag{2}$$

The spatial receptive field, $f_s(\boldsymbol{r})$, is described as a 2D Gaussian function

$$f_s(\boldsymbol{r}) = \alpha_c e^{-\ln 5 \frac{\|\boldsymbol{r}-\boldsymbol{r}_c\|^2}{R^2}}, \tag{3}$$

where $\boldsymbol{r}_c$ is the centre of the receptive field, α_c is the amplitude at the centre, and R determines the radius of the spatial receptive field. Similar to our previous work (Lian and Burkitt, 2021), the spatial receptive field of each MEC spatio-temporal grid cell is determined by randomly sampling the grid spacing, orientation and offset from some distributions. Stensola et al. (2012) showed that MEC grid cells are discretised into modules based on their grid spacings. Following the model of Neher et al. (2017), we take four discrete grid modules whose mean grid spacings are 38.8 cm, 48.4 cm, 65 cm and 98.4 cm, and mean grid orientations are $15°$, $30°$, $45°$ and $0°$, respectively. These four discrete grid modules account for 43.5%, 43.5%, 6.5%

and 6.5% of grid cells in the model, respectively. For any MEC grid cell in its module, the grid spacing is sampled from a normal distribution with mean spacing and standard deviation of 8 cm, the grid orientation is sampled from a normal distribution with mean orientation and standard deviation of $3°$, and the grid offset is sampled from a uniform distribution between 0 and the grid spacing. Because Ismakov et al. (2017) observed the variability in individual grid fields of a MEC grid cell, the amplitude (α_c in Eq 3) of each grid field for a MEC grid cell is sampled from a normal distribution with mean 1 and standard deviation 0.1 (Neher et al., 2017; Lian and Burkitt, 2021). The radius, R in Eq 3, of the receptive field is determined by $R = 0.32\lambda$, where λ is the grid spacing of the MEC grid cell. The spatial receptive field (rate map) of one example MEC grid cell is displayed in Fig 1A.

The phase modulation, $f_\phi(\boldsymbol{r}, t)$, describes the temporal response (i.e., the probability of the timing of the individual action potentials) and is given by

$$f_\phi(\boldsymbol{r}, t) = e^{k_\phi(\cos(2\pi F t - \phi(\boldsymbol{r})) - 1)}, \tag{4}$$

where k_ϕ is the parameter that controls the level of phase precession, F is the frequency of theta rhythm and set to 10 Hz throughout the paper, and $\phi(\boldsymbol{r})$ is a function that returns the firing phase at location $\boldsymbol{r}$. Fig 1B shows the dependence of phase modulation on k_ϕ. $\phi(\boldsymbol{r})$ is set to $180°$ when plotting the curve. The larger k_ϕ is, the stronger phase modulations is. When k_ϕ is 0, there is no phase modulation and the response of MEC grid cells only depends on the spatial location of the animal.

In a 1D linear track, Chadwick et al. (2015) and McClain et al. (2019) model $\phi(r)$ as a linear function of the location, r:

$$\phi(r) = \phi_0 - \Delta\phi \frac{r - r_c + R}{2R}, \tag{5}$$

where ϕ_0 is the entry phase at location $r_c - R$, $\Delta\phi$ is the phase change across the receptive field, and thus the exit phase at location $r_c + R$ is $\phi_0 - \Delta\phi$. r and r_c become scalars instead of vectors in 1D.

However, $\phi(\boldsymbol{r})$ is more complicated to be determined in a 2D environment because the animal can enter and exit the receptive field from any locations with any running directions, and the running trajectory does not always pass through the centre of the receptive field. Jeewajee et al. (2014) show that the best correlate

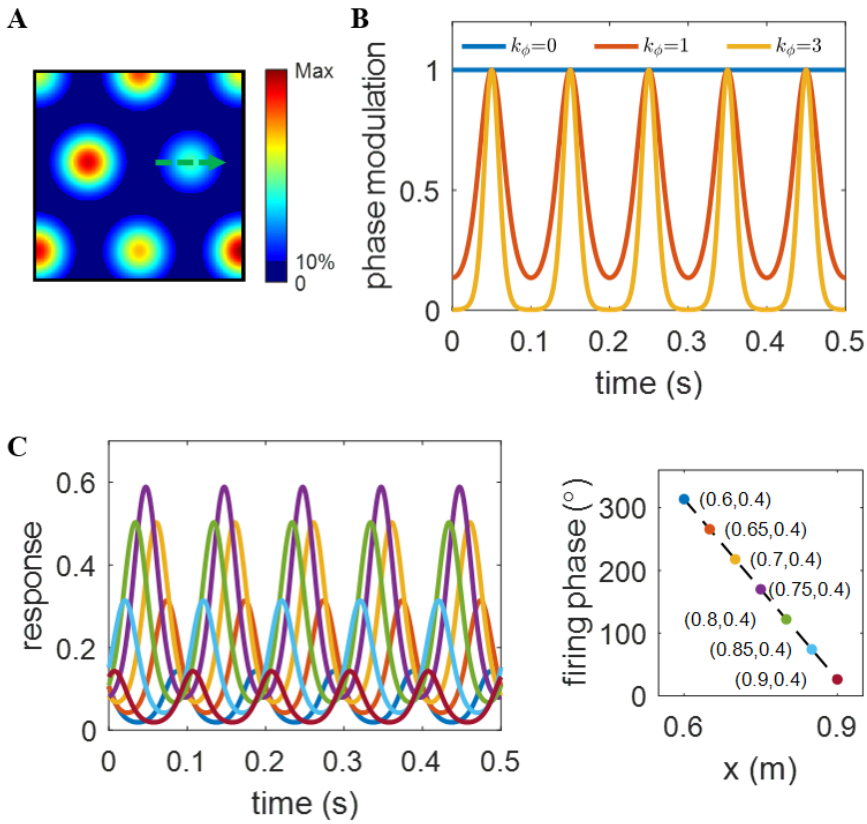

Figure 1: **Illustration of the mathematical model of a MEC spatio-temporal grid cell.** (A) The spatial receptive field (rate map), $f_s(\boldsymbol{r})$ in Eq 3, of a MEC grid cell. The green dashed arrow indicates the running trajectory used in (C). (B) Phase modulation, $f_\phi(\boldsymbol{r}, t)$ in Eq 4, for 3 different values of k_ϕ. $\phi(\boldsymbol{r})$ is set to $180°$. The response is more phase locked for larger values of k_ϕ. (C) Left: the curves in different colours represent responses of one example of learnt hippocampal place cell over 0.5 s at different locations (coordinates found in the right plot) when the animal moves from left to right of the place field along the trajectory in (A); Right: firing phase vs. position (only x varies because the animal moves from left to right). For this cell, $k_\phi = 1$, $\phi_0 = 320°$, $\Delta\phi = 300°$, $R = 0.16$ m and $F = 10$ Hz.

of phase precession in the open environment is the projected distance onto the animal's running direction. Inspired by this work, $\phi(\boldsymbol{r})$ in a 2D environment is determined by a projected version of $\phi(r)$ in Eq 5, described as:

$$\phi(\boldsymbol{r}) = \phi_0 - \Delta\phi \frac{\boldsymbol{r} - \boldsymbol{r_c}' + R'}{2R'}, \tag{6}$$

where $\boldsymbol{r_c}'$ is the projected centre and R' is the projected radius onto the running direction. In any locations within the receptive field, the firing phase $\phi(\boldsymbol{r})$ depends on the spatial location and running direction. Firing phases at the same location of different trajectories might have different values due to different running

directions.

Consequently the spatio-temporal responses of a MEC grid cells are simply modelled as multiple grid fields at all the vertices of the hexagonal grid in which each grid field is characterised by the spatio-temporal model described above (Eqs 2-6).

From Eqs 2-6, we can see that the spatio-temporal response is periodical with frequency F when the rat stays at a fixed location within the receptive field. Therefore, supposing the rat stays still at $\boldsymbol{r}$ for 1 s, the spatio-temporal response over this 1 s will be oscillating at frequency F with phase determined by $\phi(\boldsymbol{r})$ and the magnitude of the oscillating response is determined by $f_s(\boldsymbol{r})$. In other words, from the spatio-temporal response over 1 s at a fixed location, we can infer the firing phase and firing frequency of the temporal coding at the location. Though theta waves are generally absent in stationary animals (Bland, 1986), the spatio-temporal firing response over 1 s at a fixed location is used in this paper to visualise, estimate and analyse the temporal properties at different locations within the receptive field. However, it does not imply that the animal stays at any location for 1 s when freely exploring the environment. When the model is in the learning process, the animal is continually moving in a spatial environment along a trajectory generated by Eq 1. After learning, the spatio-temporal response over 1 s at different locations is used to recover the learnt temporal properties of hippocampal place cells (details found in Section 2.8 and 2.9).

The response of one example MEC spatio-temporal grid cell is illustrated in Fig 1. The spatial receptive field (rate map) of this grid cell is displayed in Fig 1A. For this cell, $k_\phi = 1$, $\phi_0 = 320°$, $\Delta\phi = 300°$ and $R = 0.16$ m. The green dashed arrow in Fig 1A indicates the trajectory the animal runs through a grid field. The left plot in Fig 1C shows the response over 0.5 s when the animal is in different locations of the running trajectory (green dashed arrow in Fig 1A) in which the coordinates of locations are given in the right plot with the same colour coding. At each location, the response over 0.5 s is intentionally plotted to visualise the spatial and temporal properties. As the animal runs from the left to the right of the grid field, the spatial response ($f_s(\boldsymbol{r})$ in Eq 3), amplitude of the periodic curve, increases, peaks at the centre, and then decreases. However, the phase of the periodic curve ($\phi(\boldsymbol{r})$ in Eqs 4 and 6) starts with a value close to 360° and then keeps decreasing along the trajectory, mimicking the theta phase precession. Theta phase precession can also be observed from the right plot of Fig 1C which shows that the curve of firing phase vs. position (x) has

a correlation coefficient -1. Note that the theta phase precession is incorporated by the temporal component that linearly varies the firing phase with the spatial location within the receptive field (Eqs 4-6). Above all, Fig 1 shows that our mathematical model of MEC spatio-temporal grid cells shows both spatial and temporal dependence, and the theta phase precession introduced here is perfect with correlation coefficient -1. We are aware that theta phase precession can never be perfect in experimental studies. However, from a modelling perspective, we can investigate how well the modelled hippocampal place cells preserve the perfect theta phase precession of MEC spatio-temporal grid cells after learning.

2.3 EC weakly spatial cells

Though MEC grid cells have a clear spatial structure, they account for roughly 20% of the MEC cell population (Diehl et al., 2017). Furthermore, Diehl et al. (2017) found that about two-thirds of MEC cells (i.e., the non-grid spatial cells) have less specialised but consistent spatial firing patterns. In addition, cells in the lateral entorhinal cortex (LEC), that contains spatial information (Hargreaves et al., 2005; Yoganarasimha et al., 2011), can also contribute to the formation of hippocampal place cells. In our previous work, we showed that a model based on sparse coding can effectively retrieve place information from EC weakly spatial cells which have no structured spatial selectivity to form an efficient hippocampal place map (Lian and Burkitt, 2021). In this paper, we incorporated EC weakly spatial cells and treated them as potential upstream input to the hippocampus to investigate how EC weakly spatial cells and MEC spatio-temporal grid cells altogether contribute to the spatial and temporal properties of hippocampal place cells. In the simulation, the firing field of EC weakly spatial cells was generated by first sampling from a uniform distribution between 0 and 1 for each location, then smoothing the map with a Gaussian kernel with a standard deviation of 6 cm, and normalising the map to give values between 0 and 0.1.

2.4 Non-negative sparse coding

Similar to our previous work (Lian and Burkitt, 2021), we build here the learning model of spatio-temporal place cells based upon non-negative sparse coding (Hoyer, 2003). Sparse coding, originally proposed by Olshausen and Field (1996, 1997), finds an efficient representation of the input using a linear combination of some basis vectors. Non-negative sparse coding constrains the responses and basis vectors to be non-

negative. We implement the model via a locally competitive algorithm (Rozell et al., 2008) that efficiently solves sparse coding as follows:

$$\begin{aligned} \tau \dot{\mathbf{u}} &= -\mathbf{u} + \mathbf{A}^T \mathbf{I} - \mathbf{W}\mathbf{s} \\ \mathbf{s} &= \max(\mathbf{u} - \beta, 0) \end{aligned} \tag{7}$$

and

$$\Delta \mathbf{A} \propto (\mathbf{I} - \mathbf{A}\mathbf{s})\mathbf{s}^T \text{ with } \mathbf{A} \geq 0, \tag{8}$$

where $\mathbf{I}$ is the input, $\mathbf{s}$ represent the response (firing rate) of the model units, $\mathbf{u}$ can be interpreted as the membrane potential, $\mathbf{A}$ is the matrix containing basis vectors and can be interpreted as the connection weights between the input and model units, $\mathbf{W} = \mathbf{A}^T\mathbf{A} - \mathbb{1}$ and can be interpreted as the recurrent connection between model units, $\mathbb{1}$ is the identity matrix, τ is the time constant, and β is the positive sparsity constant that controls the threshold of firing. Each column of $\mathbf{A}$ is normalised to have length 1. The non-negative constraints are incorporated into the system, as seen from the non-negativity of both $\mathbf{s}$ and $\mathbf{A}$ in Eqs 7 and 8. Additional details about the implementation of non-negative sparse coding can be found in Lian and Burkitt (2021).

2.5 Structure of the model

In this paper, EC provides upstream input for the hippocampus and the EC-hippocampus pathway is modelled in three scenarios. The diagram of the model structure is displayed in Fig 2. A summary of all symbols defined in this paper is shown in Table 1.

Scenario 1: modelled hippocampal place cells only receive input from MEC spatio-temporal grid cells described earlier, which have both spatial and temporal response properties (see Section 2.2). EC-hippocampus connection undergoes a learning process while the animal is exploring the environment. This scenario is designed to investigate the contribution of MEC spatio-temporal grid cells to the spatial and temporal properties of modelled hippocampal place cells.

Scenario 2: modelled hippocampal place cells receive input from MEC spatio-temporal grid cells together with EC weakly spatial cells. Similar to Scenario 1, the EC-hippocampus connection is learnt. This scenario aims to validate the results of Scenario 1 even when other spatial cells in the EC also contribute to the firing

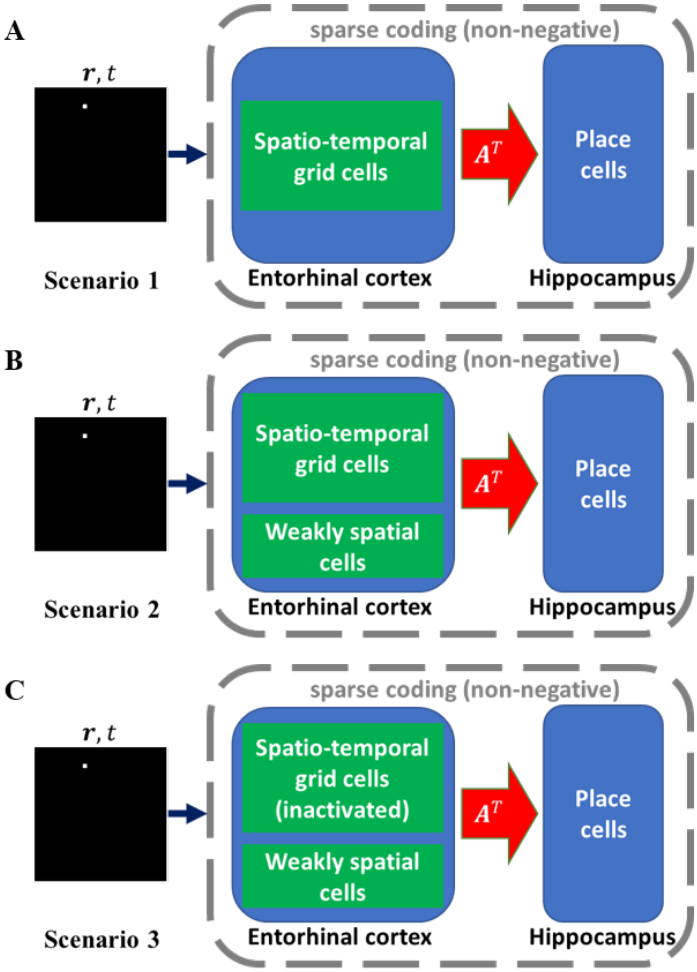

Figure 2: **Model structure in three scenarios.** MEC spatio-temporal grid cells or EC weakly spatial cells serve as the upstream input to the hippocampus. Given a spatial location $\boldsymbol{r}$ from a virtual rat running trajectory and time t, EC provides input for the hippocampus. The responses of modelled hippocampal place cells and the connection weights $\mathbf{A}$ are updated by Eqs 7 and 8. (A) Scenario 1: only MEC spatio-temporal gird cells serve as the EC input. (B) Scenario 2: both MEC spatio-temporal grid cells and EC weakly spatial cells serve as the EC input. (C) Scenario 3: MEC spatio-temporal grid cells were inactivated after the learning process of Scenario 2.

of modelled hippocampal place cells.

Scenario 3: after the learning process of Scenario 2, MEC spatio-temporal grid cells are inactivated and there is no learning in this scenario. This scenario is used to replicate the experimental setup of the study by Schlesiger et al. (2015), in which rats received NMDA lesions of the MEC. Schlesiger et al. (2015) found that theta phase precession of hippocampal place cells was greatly disrupted by MEC lesions but hippocampal spatial firing still remained. In this scenario, the spatial firing of hippocampal place cells will be investigated after the inactivation of MEC spatio-temporal grid cells.

2.6 Training

The values of training parameters and definition of symbols can be found in Table 1. As the virtual rat moves in the environment, each MEC spatio-temporal grid cell generates a firing rate that is determined by the spatial location $\boldsymbol{r}$ and time t according to Eqs 2-6, while each of the EC weakly spatial cells generates a firing rate determined only by the spatial location. The response of modelled hippocampal place cells is computed iteratively using the model dynamics (Eq 7). The connection, $\mathbf{A}$, between EC cells and modelled hippocampal place cells is updated according to the learning rule described in Eq 8. There are 100 modelled hippocampal place cells in the model and three different scenarios are implemented.

Scenario 1: only MEC spatio-temporal grid cells provide input to the modelled hippocampal place cells, there are 900 MEC spatio-temporal grid cells, i.e., $\mathbf{A}$ is a 900×100 matrix. A running trajectory of 3600 s is used to train the model and connection, $\mathbf{A}$, is learnt during this training process.

Scenario 2: both MEC spatio-temporal grid cells and EC weakly spatial cells provide input for the hippocampus. Besides the 900 MEC spatio-temporal grid cells, there are also 400 EC weakly spatial cells; i.e., $\mathbf{A}$ is a 1300×100 matrix where the top 400 rows of $\mathbf{A}$ represent the connection weights from EC weakly spatial cells to modelled hippocampal place cells and the bottom 900 rows represent the connection weights from MEC grid cells to modelled hippocampal place cells. The same running trajectory of 3600 s, as used in Scenario 1, is used to train the model.

Scenario 3: after the learning process in Scenario 2, MEC spatio-temporal grid cells were inactivated in order to investigate how this affects the spatial firing of modelled hippocampal place cells after temporal

input from MEC grid cells is lost. MEC grid cells are inactivated by setting the bottom 900 rows of $\mathbf{A}$ (the connection weights from MEC spatio-temporal grid cells to modelled hippocampal place cells) to zero and then normalising each column of $\mathbf{A}$ to have length 1. In this scenario, there is no learning.

$\mathbf{A}$ is initialised according to a uniform distribution between 0 and 1 and then normalised to have length 1 for each column. For both Scenario 1 and 2, a running trajectory of 3600 s is used to train the model and connection, $\mathbf{A}$, is learnt during this training process. After learning, another running trajectory of 1200 s is used to recover the spatial receptive fields or investigate the temporal properties of these 100 modelled hippocampal place cells for all three scenarios.

The parameters in Eqs 4 and 6 that control the temporal properties of MEC grid cells are chosen as follows: k_ϕ is chosen randomly from a uniform distribution between 0.8 and 1.2; ϕ_0 and $\Delta\phi$ are both chosen randomly from a uniform distribution between 300° and 340°; and F is 10 Hz.

For the parameters in the model dynamics and learning rule (Eqs 7 and 8), τ is 10 ms, β is 0.3, and the time step of computing modelled hippocampal place cells by Eq 7 is taken to be 0.2 ms. Because the trajectory is updated after every 10 ms, there are 50 iterations of computing the responses of modelled hippocampal place cell using Eq 7. The learning rate of updating the connection, $\mathbf{A}$, is 0.01.

2.7 Recovering the spatial receptive fields of modelled hippocampal place cells

After training, another running trajectory of the virtual rat with a duration of 1200 s was used to recover the spatial receptive fields (rate maps) of modelled hippocampal place cells. The 1m$\times$1m environment is discretised into a 40$\times$40 lattice and the receptive field is recovered as the averaged response across all locations along the running trajectory of 1200 s.

2.7.1 Fitting the spatial receptive fields

In order to quantitatively characterise the spatial receptive fields of learnt hippocampal place cells, the recovered receptive fields using the approach above is fitted by the following function:

$$\hat{f}_s(\boldsymbol{r}) = \hat{\alpha}_c e^{-\ln 5 \frac{\|\boldsymbol{r}-\hat{\boldsymbol{r}}_c\|^2}{\hat{R}^2}}, \tag{9}$$

where $\hat{\alpha}_c$ is the amplitude, $\hat{\boldsymbol{r}}_c$ is the centre and $\hat{R}$ determines the radius of the receptive field. The fitting routine is performed using the built-in MATLAB (version R2020a) function *lsqcurvefit* and the fitting error is defined as the ratio between the summed square of the fitting residual and the summed square of the recovered receptive field.

2.7.2 Selecting place cells

The criteria of categorising a modelled hippocampal place cell as a place cell are: (1) The centre, $\hat{\boldsymbol{r}}_c$, is inside the spatial environment (2) The radius, $\hat{R}$, is larger than 5 cm (3) The fitting error is smaller than 40%, where the fitting error is defined as the square of the ratio between the fitting residual and spatial field. The receptive field of a place cell is called the *place field*. These two criteria are designed to preserve learnt hippocampal place cells that have a reasonable size of the place field and only one dominant place field.

2.8 Fitting the spatio-temporal response of modelled hippocampal place cells

The MEC spatio-temporal grid cells in the model have built-in spatial and temporal properties as described in Eqs 2-6, so their responses at a fixed position over 1 s display the periodic pattern illustrated in Fig 1. However, modelled hippocampal place cells have neither built-in spatial nor temporal properties. After learning, the responses of hippocampal place cells are determined by the model dynamics (Eq 7) where $\mathbf{A}$ is learnt during the (virtual) rat navigation. To investigate the temporal properties of learnt hippocampal place cells, the responses of hippocampal place cells over 1 s at a given location is fitted to the following function:

$$\hat{f} = \hat{\alpha} e^{\hat{k}_\phi \left(\cos\left(2\pi \hat{F} t - \hat{\phi}\right)\right) - 1)}, \tag{10}$$

where $\hat{f}$ is the fitted responses, $\hat{\alpha}$ is the fitted amplitude that represents the spatial firing rate at this location, $\hat{k}_\phi$ is the estimated parameter that controls the level of dependence on phase precession, $\hat{F}$ is the estimated frequency of the response, and $\hat{\phi}$ is the estimated phase of the response. The fitting routine is performed using the built-in MATLAB (version R2020a) function *lsqcurvefit*. The fitting error is defined as the square of the ratio between the fitting residual and original response.

2.9 Measuring the temporal properties of modelled hippocampal place cells

In order to quantitatively investigate the temporal properties of the theta phase precession of learnt hippocampal place cells, the following approach was used. First, for the modelled hippocampal place cells that meet the criteria of a place cell described earlier (Section 2.7.2), only cells whose entire place fields lie in the spatial environment are considered. Second, for each hippocampal place cell, a random running direction is uniformly sampled between 0 and 360° and then a straight trajectory passing the place field centre with this random running direction is generated. Third, the response over 1 s at each position along the straight trajectory is generated by the model and then fitted using Eq 10. Finally, the entry phase, exit phase, and correlation coefficient between firing phases and positions are obtained. For a hippocampal place cell with theta phase precession, entry phase should be large and close to 360°, exit phase should be small and close to 0°, and the correlation coefficient between firing phases and positions should be negative and close to -1.

3 Results

3.1 Scenario 1: the spatio-temporal properties of hippocampal place cells can be inherited from MEC grid cells via plasticity

The results presented here are those from Scenario 1, namely the simulation in which only MEC spaio-temporal grid cells provide input for the modelled hippocampal place cells. The MEC spatio-temporal grid cell to place cell connectivity was learnt using non-negative sparse coding over 3600 s of virtual rat navigation over the 1 m $\times$ 1 m environment, as described in Section 2.6. Through this training, the modelled hippocampal place cells learn to pool different MEC spatio-temporal grid cells in such a way that the place cells become selective to specific locations in the spatial environment. The receptive fields of the 94 out of 100 modelled hippocampal place cells that meet the criteria for place cells described in Section 2.7.2 are plotted in Fig 3A. These learnt hippocampal place cells have a dominant firing location and their firing locations differ from each other. The centres of each of these 94 place fields are displayed in Fig 3B, which are estimated using Eq 9. This figure shows that the population of learnt hippocampal place cells tile the entire spatial environment in a fairly uniform fashion. Compared with our previous work (Figure 3 in Lian and Burkitt (2021)), the tiling of the hippocampal place cells here is less uniform due to the lack of

uniformity in the rat running trajectory.

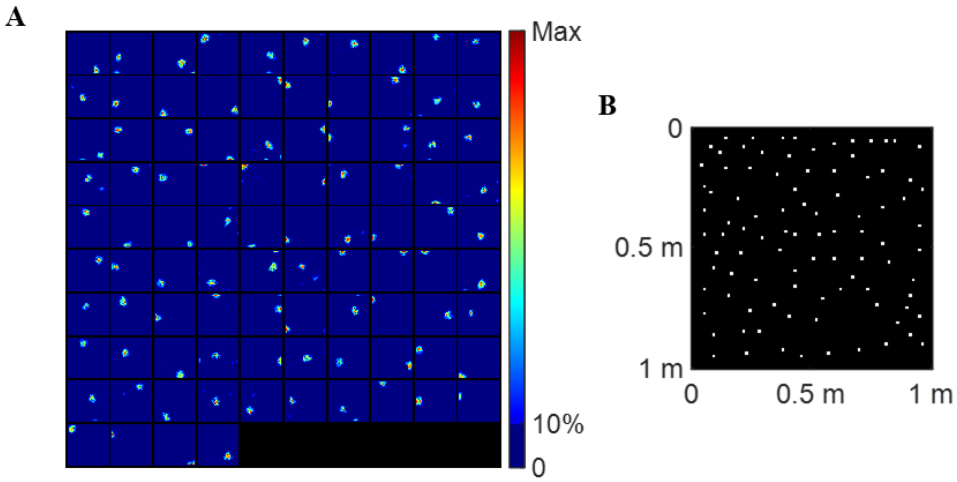

Figure 3: **Scenario 1: learnt hippocampal place cells display spatial properties.** (A) Place fields of 94 (out of 100) learnt hippocampal place cells that passed the criteria of place cell. Each block represents the spatial receptive field (rate map) of a cell in a 1m×1m environment. (B) Centres of these 94 learnt hippocampal place cells plotted together in the 1m $\times$ 1m environment. Values of parameters used in the simulation can be found in Table 1.

Furthermore, these learnt hippocampal place cells also display the temporal property of theta phase precession. This is illustrated in the response of a learnt hippocampal place cell over 0.5 s shown in Fig 4.

Similar to Fig 1A, Fig 4A shows the response of one learnt hippocampal place cell over 0.5 s at position $(0.65, 0.75)$, which is the centre of the place field (right plot). The solid line in the left plot represents the response of this example place cell over 0.5 s and displays a periodic pattern. After fitting the response of the learnt place cell to the spatio-temporal function described by Eq 10, the fitted response is plotted in the dashed line. The response of this learnt place cell is well fitted by Eq 10 and the fitting error is as small as 0.35%. The fitted parameters are $\hat{\alpha} = 2.68$, $\hat{k}_\phi = 0.69$, $\hat{F} = 10.00$ Hz and $\hat{\phi} = 177.77°$.

The response of the same example place cells over 0.5 s as the animals runs from left to right of the place field (through the field centre) is shown in Fig 4B. As the animal is at position $(0.5, 0.75)$, the amplitude of the response curve is below 1 and the firing phase (indicated by the peak location) is close to the end of each cycle (i.e., late phase). As the animal continues running to the right, the amplitude of the response curve increases and then decreases, while the firing phase continues to shift forward to the beginning of each

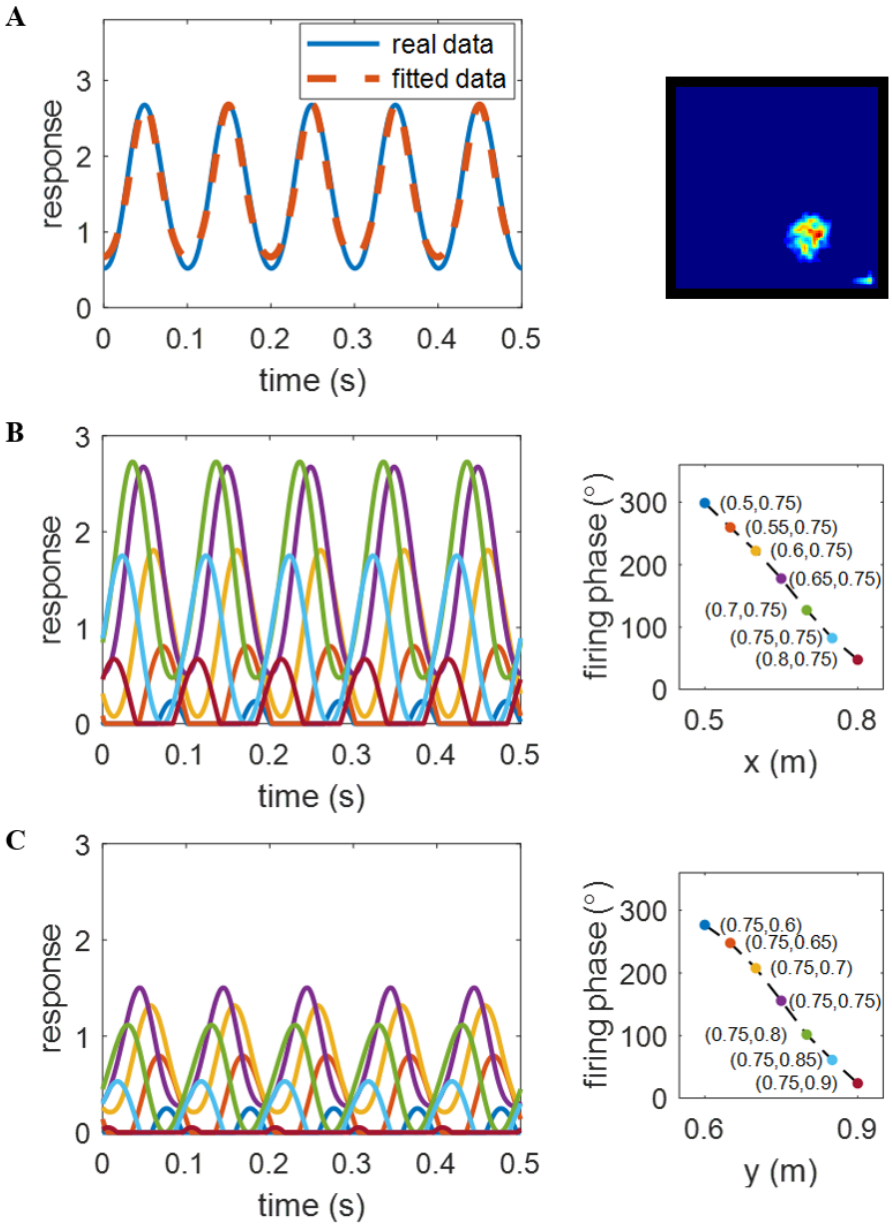

Figure 4: **Scenario 1: one example of learnt hippocampal place cells displays temporal properties.** (A) Left: the response (solid line) over 0.5 s at the centre of the place field and the fitted response (dashed line) by Eq. 10; Right: rate map of this example place cell whose centre is at $(0.65, 0.75)$. (B) Left: the curves in different colours represent responses of this learnt hippocampal place cell over 0.5 s at different locations (coordinates found in the right plot) when the animal moves from left to right of the place field; Right: firing phase vs. position (only x varies because the animal moves from left to right). (C) Left: the curves in different colours represent responses of this learnt hippocampal place cell over 0.5 s at different locations (coordinates found in the right plot) when the animal moves from top to bottom of the place field (not through the field centre); Right: firing phase vs. position (only y varies because the animal moves from top to bottom). Values of parameters used in the simulation can be found in Table 1.

cycle. After fitting the response curve by Eq 10, the relationship between firing phase and position is shown in the inset plot of Fig 4B, which shows a clear correlation; namely that the firing phase moves from late phase to early phase as the animal crosses the place field. The entry phase and exit phase are 303.9° and 28.7°, respectively. The correlation coefficient between firing phases and positions is -0.998. Therefore, as the animal runs from the left to the right of the place field, this place cell response displays theta phase precession. In other words, after learning, the resulting hippocampal place cells not only display spatial place fields but also display phase precession.

The learnt place cell also displays theta phase precession when the animal crosses the place field in another direction: This is illustrated in Fig 4C, in which the animal moves from top to bottom but not through the centre of the place field. This response is similar to that previously shown in Fig 4B. The amplitude of the response curve is small when the animal enters the place field, increases to the peak when the animal is near the place field centre, and then decreases as the animal moves away from the place field centre. The firing phase is observed to shift from late phase to early phase; i.e., displaying theta phase precession. The entry phase is 302.9°, exit phase is 17.6°, and the correlation coefficient between firing phases and positions is -0.997.

Consequently the example place cell in Fig 4 learns both spatial and temporal properties after training. These spatio-temporal properties for the modelled hippocampal place cells are not inherent properties of the place cells, but arise entirely due to the way in which the model learns a place specific tuning and theta phase precession from the spatio-temporal information provided by the MEC grid cells.

Among the 94 (out of 100) hippocampal place cells, 58 place cells have their entire place fields inside the spatial environment. The population statistics of the temporal properties are shown in Fig 5. Fig 5A and B show that the firing phase of these cells is at a late phase when the animal enters the place field and at an early phase when the animal leaves the place field. The histogram of their correlation coefficient between the entry and exit phases in Fig 5C demonstrates that the firing phase is strongly reverse-correlated with the position within the place field, indicating strong theta phase precession. Recall that the MEC grid cells are constructed here to have this built-in phase precession property (characterised by Eq 4-6). For each grid field of the MEC grid cell the firing phase and position along a straight trajectory are constructed to be have a

correlation coefficient of -1 due of the linear relationship between the firing phase and position (Eq 6). Both the spatial and temporal response properties of the hippocampal place cells are entirely learnt from pooling the input they receive from MEC grid cells. Furthermore, the fact that the correlation coefficients in Fig 5 are very close to -1 indicates that theta phase precession is well preserved in the learnt hippocampal place cells.

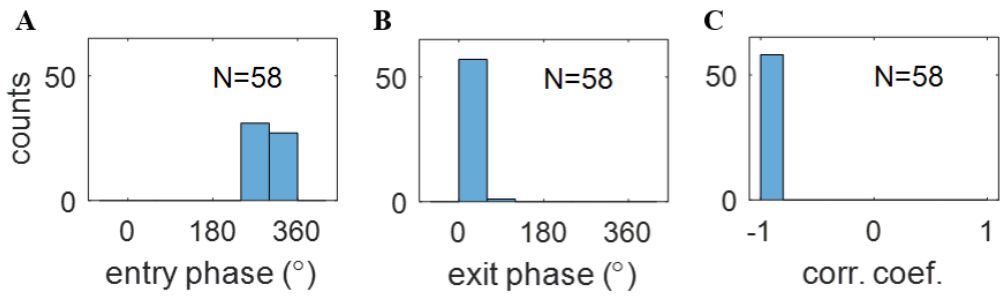

Figure 5: **Scenario 1: the population of learnt hippocampal place cells displays temporal properties.** Histograms of the entry phases (A), exit phase (B), and correlation coefficient (C) show that learnt hippocampal place cells have strong theta phase precession. Values of parameters used in the simulation can be found in Table 1.

3.2 Scenario 2: the spatio-temporal properties of hippocampal place cells can be learnt when both MEC grid cells and EC weakly spatial cells serve as the EC input to the hippocampus

In this section, we show the results of training with Scenario 2: namely where both MEC spatio-temporal grid cells and EC weakly spatial cells provide input for the modelled hippocampal place cells. The results show that both MEC grid cells and EC weakly spatial cells provide spatial information for the hippocampus, so that a spatial hippocampal map can be retrieved from upstream input, while MEC grid cells provide temporal information that results in theta phase precession also being inherited from upstream.

A demonstration of how EC weakly spatial cells and MEC grid cells contribute to the spatial and temporal properties of hippocampal place cells is given in Fig 6. After learning, the recovered rate maps show place-field like receptive fields. As seen from Fig 6A, different hippocampal place cells learn different place fields and the hippocampal population tiles the entire environment, similar to Scenario 1 where only MEC grid cells provide input for the hippocampus (Fig 3). An example of the temporal response properties of a place

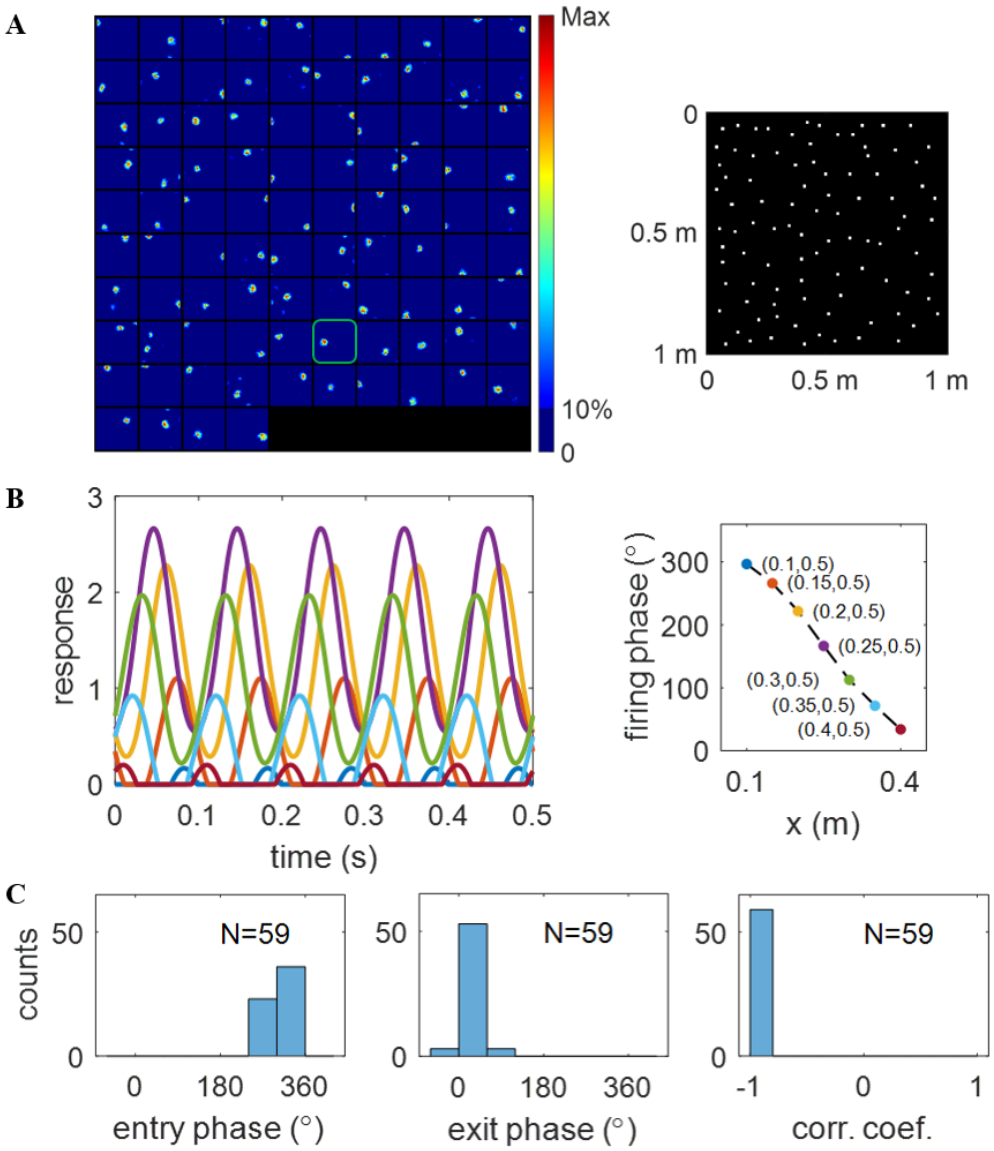

Figure 6: **Scenario 2: learnt hippocampal place cells display spatio-temporal properties.** (A) Spatial properties of learnt hippocampal place cells. Left: the place fields of learnt hippocampal place cells; Right: their centres plotted in the same environment. (B) Illustration of theta phase precession for one learnt hippocampal place cells highlighted in (A). Left: the curves in different colours represent responses of this learnt place cell over 0.5 s at different locations (coordinates found in the right plot) when the animal moves from left to right of the place field; Right: firing phase vs. position (only x varies because the animal moves from left to right). (C) The population of learnt hippocampal place cells displays temporal properties. Histograms of entry phase (Left), exit phase (Middle), and correlation coefficient (Right) indicate a strong phase precession for the learnt hippocampal place cells. Values of parameters used in the simulation can be found in Table 1.

cell is given in Fig 6B, which displays characteristic theta phase precession. As the animal moves from left to right of the place field, the amplitude of firing increases and then decreases while the firing phase shifts smoothly from a late phase to an early phase. This relationship between firing phase and position within the place field is also shown in the right plot of Fig 6B. Fig 6C displays the population statistics for this phase precession, similar to Fig 5, suggesting that learnt hippocampal place cells display strong phase precession.

3.3 Scenario 3: spatial properties of hippocampal place cells are maintained after the inactivation of MEC grid cells

After the learning process in Scenario 2, MEC spatio-temporal grid cells in the model were inactivated; i.e., only the remaining EC weakly spatial cells provide spatial information for the hippocampal place cells and there is no temporal information sent by MEC spatio-temporal grid cells. Recall that there is no learning in Scenario 3, so the spatial tuning of hippocampal place cells depends on the connectivity between EC weakly spatial cells and hippocampal place cells learnt in Scenario 2.

However, the learnt connection between EC weakly spatial cells and place cells is sufficient to maintain the place field of modelled hippocampal place cells after MEC inactivation. After recovering the receptive fields of modelled hippocampal cells (see Section 2.7), 87 out of 100 hippocampal cells were found to meet the criteria of a place cell. The place fields, along with their field centres are plotted in Fig 7A. Compared with Fig 6A, the place fields can still maintain their firing locations so that the population still tiles the entire spatial environment, suggesting that the learnt connection from EC weakly spatial cells to place cells during free running provides sufficient spatial information such that stable place fields will not be lost even though MEC grid cells are inactivated.

There are 94 place cells before inactivating MEC grid cells (Fig 6A, Scenario 2) and 87 place cells after the inactivation (Fig 7A, Scenario 3). We find that all these 87 place cells that pass the criteria after MEC inactivation (Scenario 3) come from the population of 94 place cells before MEC inactivation (Scenario 2). After inactivating the MEC grid cells, Fig 7B shows that, in general, the size of the place fields increases. Furthermore, although most place cells maintain stable place fields after the inactivation, their field centres shift randomly within a small range, as seen in Fig 7C. These results also suggest that the place coding of

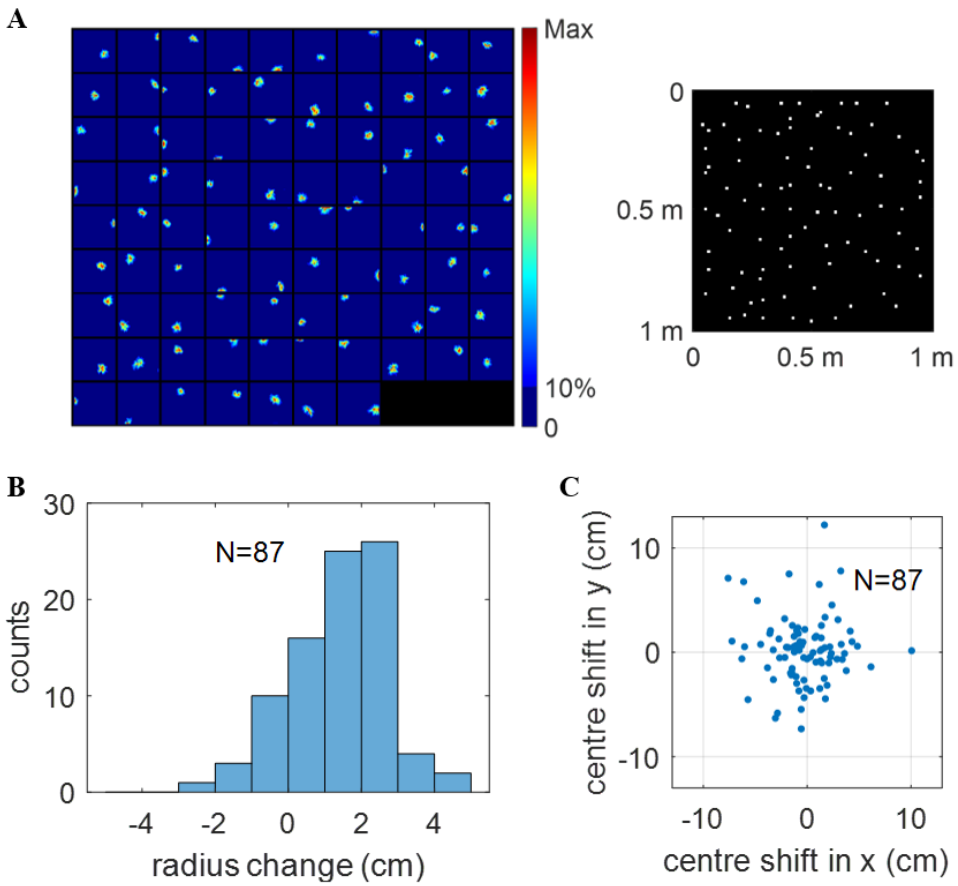

Figure 7: **Scenario 3: learnt hippocampal place cells maintain spatial firing after MEC inactivation.** (A) The place fields of 87 hippocampal place cells (Left) and their centres plotted in the same environment (Right). (B) Histogram of radius change of place fields after MEC inactivation. The radius of most place fields increases after MEC inactivation. The mean radii before and after MEC inactivation are 8.94 cm and 10.34 cm, respectively. (C) Scatter plot of the place field centre shift after MEC inactivation.

the hippocampus becomes less accurate after MEC activation.

This result is consistent with the experimental study by Schlesiger et al. (2015) who found that after MEC lesions in rats, theta phase precession of hippocampal CA1 cells was significantly disrupted, although stable spatial firing was maintained. Therefore, during the navigation of the rat in Scenario 2, the plasticity of the model allows hippocampal place cells to pool the input from upstream neurons, namely the EC weakly spatial cells or MEC grid cells, enabling both spatial and temporal properties to be learnt.

Combining results in this paper and our previous work (Lian and Burkitt, 2021), the contribution of the EC to the firing of hippocampal place cells can be described as follows: both EC weakly spatial cells and cells

with a clear structure (such as MEC grid cells) provide spatial information for the hippocampus to learn an efficient hippocampal place map, while the temporal response properties involving theta phase precession of hippocampal place cells is inherited from MEC grid cells via learning during navigation.

4 Discussion

In this study a model based on sparse coding is built that demonstrates that the spatial and temporal properties of hippocampal place cells can be learnt simultaneously via plasticity as the animal freely explores an open environment. In the training phase, a virtual rat runs for 3600 s and the connectivity matrix, $\mathbf{A}$, is learnt during this exploration period. After learning, $\mathbf{A}$ is kept fixed and another running trajectory of 1200 s is used to recover the place fields of learnt place cells. In addition, responses over 0.5 s at different positions across the place field are used to investigate the firing phases when the animal traverses the place field. Our results show that the learnt hippocampal place cells are selective to a single firing location and display theta phase precession, even though the modelled hippocampal place cells have no pre-built spatial and temporal properties. Furthermore, the model shows that the loss of MEC grid cells causes the loss of the temporal response properties of hippocampal place cells. The spatial properties of hippocampal place cells are maintained by other upstream cells, such as EC weakly spatial cells, that provide spatial information for the hippocampus. This model demonstrates how the spatio-temporal properties of hippocampal place cells can be learnt.

4.1 The entorhinal-hippocampal loop

Early computational models of place cells were mostly based upon a feedforward structure, where cells in the EC provide spatial input to the hippocampus (Solstad et al., 2006; Franzius et al., 2007b,a; de Almeida et al., 2009). Some more recent studies have adopted a loop network structure in which cells in the EC project to the hippocampus and also receive feedback from it (Rennó-Costa and Tort, 2017; Li et al., 2020; Agmon and Burak, 2020). Models incorporating this loop network structure can explain more experiment observations, especially on how hippocampal place cells affect the firing of MEC grid cells. Since the hippocampus receives information from different brain areas via the EC, place cells in the hippocampus can still maintain some properties even when MEC grid cells are inactivated. Therefore, the feedback from the hippocampus

to the EC can modify some properties of EC cells, which can only be investigated using the loop network structure. However, the results presented here does not rule out the probability of implementing the model in a loop structure because sparse coding can be implemented in a feedforward-feedback loop Lian et al. (2019).

4.2 Evidence against feedforward grid-to-place models

Recent research has provided experimental evidence that place fields emerge earlier in development than MEC grid cells (Langston et al., 2010; Wills et al., 2010). There is also experimental evidence for the maintenance of stable place fields after the inactivation of MEC grid cells (Koenig et al., 2011; Brandon et al., 2014; Schlesiger et al., 2015; Hales et al., 2014). These results put into question the feedforward nature of grid-to-place cell models.

However, the results presented in this paper, together with our previous work (Lian and Burkitt, 2021), provides a unifying framework that is able to explain this experimental evidence while supporting a hierarchical structure of connectivity from the EC to the hippocampus in which theta phase precession of hippocampal place cells is essentially inherited from MEC gird cells via learning.

4.3 Future work

While this study offers a picture of how the EC contributes to the spatial and temporal properties of hippocampal place cell, there remain a number of interesting outstanding questions to be addressed. First, the question of how the feedback from the hippocampus to the EC affects properties of EC cells remains unclear. Second, the model proposed here demonstrates how sparse coding can learn spatio-temporal properties of hippocampal place cells, but whether the principle of sparse coding can be used to explain other aspects of hippocampal function, such as those involving memory consolidation, remains unclear. In addition, the spatio-temporal model of the MEC grid cells is assumed here, and the question of how this MEC spatio-temporal grid cell structure originates is a topic of ongoing research. Moreover, the model presented here uses rate-based neurons, a spiking implementation together with spike timing dependent plasticity of this model is left for future research.

References

Agmon H, Burak Y (2020) A theory of joint attractor dynamics in the hippocampus and the entorhinal cortex accounts for artificial remapping and grid cell field-to-field variability. *eLife* 9:e56894.

Bland BH (1986) The physiology and pharmacology of hippocampal formation theta rhythms. *Prog. Neurobiol.* 26:1–54.

Brandon MP, Koenig J, Leutgeb JK, Leutgeb S (2014) New and distinct hippocampal place codes are generated in a new environment during septal inactivation. *Neuron* 82:789–796.

Bush D, Barry C, Burgess N (2014) What do grid cells contribute to place cell firing? *Trends Neurosci.* 37:136–145.

Chadwick A, van Rossum MC, Nolan MF (2015) Independent theta phase coding accounts for ca1 population sequences and enables flexible remapping. *eLife* 4:e03542.

de Almeida L, Idiart M, Lisman JE (2009) The input–output transformation of the hippocampal granule cells: from grid cells to place fields. *J. Neurosci.* 29:7504–7512.

Diehl GW, Hon OJ, Leutgeb S, Leutgeb JK (2017) Grid and nongrid cells in medial entorhinal cortex represent spatial location and environmental features with complementary coding schemes. *Neuron* 94:83–92.

D'Albis T, Kempter R (2017) A single-cell spiking model for the origin of grid-cell patterns. *PLoS Comput. Biol.* 13:e1005782.

Fiete IR, Burak Y, Brookings T (2008) What grid cells convey about rat location. *J. Neurosci.* 28:6858–6871.

Franzius M, Sprekeler H, Wiskott L (2007a) Slowness and sparseness lead to place, head-direction, and spatial-view cells. *PLoS Comput. Biol.* 3:e166.

Franzius M, Vollgraf R, Wiskott L (2007b) From grids to places. *J. Comput. Neurosci.* 22:297–299.

Hafting T, Fyhn M, Bonnevie T, Moser MB, Moser EI (2008) Hippocampus-independent phase precession in entorhinal grid cells. *Nature* 453:1248–1252.

Hafting T, Fyhn M, Molden S, Moser MB, Moser EI (2005) Microstructure of a spatial map in the entorhinal cortex. *Nature* 436:801–806.

Hales JB, Schlesiger MI, Leutgeb JK, Squire LR, Leutgeb S, Clark RE (2014) Medial entorhinal cortex lesions only partially disrupt hippocampal place cells and hippocampus-dependent place memory. *Cell Reports* 9:893–901.

Hargreaves EL, Rao G, Lee I, Knierim JJ (2005) Major dissociation between medial and lateral entorhinal input to dorsal hippocampus. *Science* 308:1792–1794.

Hoyer PO (2003) Modeling receptive fields with non-negative sparse coding. *Neurocomputing* 52:547–552.

Ismakov R, Barak O, Jeffery K, Derdikman D (2017) Grid cells encode local positional information. *Curr. Biol.* 27:2337–2343.

Jeewajee A, Barry C, Douchamps V, Manson D, Lever C, Burgess N (2014) Theta phase precession of grid and place cell firing in open environments. *Phil. Trans. R. Soc. B* 369:20120532.

Kloosterman F, Van Haeften T, Witter MP, Lopes da Silva FH (2003) Electrophysiological characterization of interlaminar entorhinal connections: an essential link for re-entrance in the hippocampal–entorhinal system. *Eur. J. Neurosci.* 18:3037–3052.

Koenig J, Linder AN, Leutgeb JK, Leutgeb S (2011) The spatial periodicity of grid cells is not sustained during reduced theta oscillations. *Science* 332:592–595.

Langston RF, Ainge JA, Couey JJ, Canto CB, Bjerknes TL, Witter MP, Moser EI, Moser MB (2010) Development of the spatial representation system in the rat. *Science* 328:1576–1580.

Leutgeb JK, Leutgeb S, Moser MB, Moser EI (2007) Pattern separation in the dentate gyrus and CA3 of the hippocampus. *Science* 315:961–966.

Li T, Arleo A, Sheynikhovich D (2020) Modeling place cells and grid cells in multi-compartment environments: Entorhinal–hippocampal loop as a multisensory integration circuit. *Neural Netw.* 121:37–51.

Lian Y, Burkitt AN (2021) Learning an efficient hippocampal place map from entorhinal inputs using non-negative sparse coding. *eNeuro* .

Lian Y, Grayden DB, Kameneva T, Meffin H, Burkitt AN (2019) Toward a biologically plausible model of LGN-V1 pathways based on efficient coding. *Front. Neural Circuits* 13:13.

McClain K, Tingley D, Heeger DJ, Buzsáki G (2019) Position–theta-phase model of hippocampal place cell activity applied to quantification of running speed modulation of firing rate. *Proc. Natl. Acad. Sci.* 116:27035–27042.

Naber PA, Lopes da Silva FH, Witter MP (2001) Reciprocal connections between the entorhinal cortex and hippocampal fields ca1 and the subiculum are in register with the projections from ca1 to the subiculum. *Hippocampus* 11:99–104.

Neher T, Azizi AH, Cheng S (2017) From grid cells to place cells with realistic field sizes. *PLoS ONE* 12:1–27.

O'Keefe J, Dostrovsky J (1971) The hippocampus as a spatial map: preliminary evidence from unit activity in the freely-moving rat. *Brain Res.* 34:171–175.

O'Keefe J, Recce ML (1993) Phase relationship between hippocampal place units and the EEG theta rhythm. *Hippocampus* 3:317–330.

Olshausen BA, Field DJ (1996) Emergence of simple-cell receptive field properties by learning a sparse code for natural images. *Nature* 381:607–609.

Olshausen BA, Field DJ (1997) Sparse coding with an overcomplete basis set: A strategy employed by V1? *Vision Res.* 37:3311–3325.

Park E, Dvorak D, Fenton AA (2011) Ensemble place codes in hippocampus: CA1, CA3, and dentate gyrus place cells have multiple place fields in large environments. *PLoS ONE* 6:e22349.

Rennó-Costa C, Tort AB (2017) Place and grid cells in a loop: implications for memory function and spatial coding. *J. Neurosci.* 37:8062–8076.

Rolls ET, Stringer SM, Elliot T (2006) Entorhinal cortex grid cells can map to hippocampal place cells by competitive learning. *Network* 17:447–465.

Rozell CJ, Johnson DH, Baraniuk RG, Olshausen BA (2008) Sparse coding via thresholding and local competition in neural circuits. *Neural Comput.* 20:2526–2563.

Savelli F, Knierim JJ (2010) Hebbian analysis of the transformation of medial entorhinal grid-cell inputs to hippocampal place fields. *J. Neurophysiol.* 103:3167–3183.

Schlesiger MI, Cannova CC, Boublil BL, Hales JB, Mankin EA, Brandon MP, Leutgeb JK, Leibold C, Leutgeb S (2015) The medial entorhinal cortex is necessary for temporal organization of hippocampal neuronal activity. *Nat. Neurosci.* 18:1123–1132.

Slomianka L, Amrein I, Knuesel I, Sørensen JC, Wolfer DP (2011) Hippocampal pyramidal cells: the reemergence of cortical lamination. *Brain Struct. Funct.* 216:301–317.

Soderstrand MA, Jenkins WK, Jullien GA, Taylor FJ (1986) *Residue number system arithmetic: modern applications in digital signal processing* New York: IEEE.

Solstad T, Moser EI, Einevoll GT (2006) From grid cells to place cells: a mathematical model. *Hippocampus* 16:1026–1031.

Stensola H, Stensola T, Solstad T, Frøland K, Moser MB, Moser EI (2012) The entorhinal grid map is discretized. *Nature* 492:72–78.

Steward O, Scoville SA (1976) Cells of origin of entorhinal cortical afferents to the hippocampus and fascia dentata of the rat. *J. Comp. Neurol.* 169:347–370.

Tamamaki N, Nojyo Y (1993) Projection of the entorhinal layer II neurons in the rat as revealed by intracellular pressure-injection of neurobiotin. *Hippocampus* 3:471–480.

Wills TJ, Cacucci F, Burgess N, O'Keefe J (2010) Development of the hippocampal cognitive map in preweanling rats. *Science* 328:1573–1576.

Yoganarasimha D, Rao G, Knierim JJ (2011) Lateral entorhinal neurons are not spatially selective in cue-rich environments. *Hippocampus* 21:1363–1374.

Zhang SJ, Ye J, Miao C, Tsao A, Cerniauskas I, Ledergerber D, Moser MB, Moser EI (2013) Optogenetic dissection of entorhinal-hippocampal functional connectivity. *Science* 340:1232627.